Structural Characteristics of the Nucleotide-Binding Site of *Escherichia coli* Primary Replicative Helicase DnaB Protein. Studies with Ribose and Base-Modified Fluorescent Nucleotide Analogs†

Wlodzimierz Bujalowski* and Malgorzata Maria Klonowska‡

Department of Human Biological Chemistry & Genetics, The University of Texas Medical Branch at Galveston, Galveston, Texas 77555-0653

Received January 5, 1994; Revised Manuscript Received February 15, 1994®

ABSTRACT: Structural characteristics of the base- and ribose-binding regions of the high-affinity noninteracting nucleotide-binding site of *Escherichia coli* primary replicative helicase DnaB protein have been studied, using the base-modified fluorescent nucleotide analog 1, N^6-ethenoadenosine diphosphate (εADP) and the ribose-modified fluorescent analogs 3′(2′)-*O*-(*N*-methylantraniloyl)adenosine 5′-diphosphate (MANT-ADP), 3′-*O*-(*N*-methylantraniloyl)deoxyadenosine 5′-diphosphate (MANT-dADP), 3′-*O*-(*N*-methylantraniloyl)-deoxyadenosine 5′-triphosphate (MANT-dATP), and 2′(3′)-*O*-(2,4,6-trinitrophenyl)adenosine 5′-diphosphate (TNP-ADP). The obtained data indicate contrasting differences between these two regions. Binding of εADP to the DnaB helicase causes only ~21% increase of the nucleotide fluorescence intensity and no shift of the emission spectrum maximum. The fluorescence of bound εADP is characterized by a single lifetime of 24.2 ± 0.6 ns, only slightly shorter than the fluorescent lifetime of the free εADP in solution (25.5 ± 0.6 ns). Solute-quenching studies of bound εADP, using different quenchers, acrylamide, I^-, and Tl^+, indicate limited accessibility of ethenoadenosine to the solvent. These results strongly suggest that the base-binding region of the DnaB nucleotide-binding site is located in the polar cleft on the enzyme's surface. Moreover, the limiting emission anisotropy of bound εADP is 0.21 ± 0.02, compared to the anisotropy of 0.3 of completely immobilized εADP at the same excitation wavelength (λ_{ex} = 325 nm, λ_{em} = 410 nm), indicating that the adenine preserves substantial mobility when bound in the base-binding site. In contrast, fluorescence intensity at the emission maximum of TNP-ADP and MANT-ADP, which has modifying groups attached to the 2′ and/or 3′ oxygens of the ribose, increases upon binding to DnaB by factors of ~4.7 (λ_{ex} = 408 nm) and ~2.6 (λ_{ex} = 356 nm), respectively. Moreover, the maximum of emission spectrum of bound TNP-ADP is blue-shifted by ~11 nm and that of MANT-ADP by ~12 nm. Comparisons between spectral properties of TNP-ADP and MANT-ADP bound to DnaB and in different solvents suggest that the ribose-binding region of the DnaB nucleotide-binding site has relatively low polarity. Solute quenching studies of MANT-ADP fluorescence, using acrylamide, I^-, and Tl^+, indicate that the MANT group has very little accessibility to the solvent when bound to DnaB. Taken together, these results suggest that the ribose-binding region constitutes a hydrophobic cleft, or pocket, with very limited, if any, contact with the solvent. Moreover, fluorescence anisotropy of bound TNP-ADP and MANT-ADP is 0.32 ± 0.02 and 0.33 ± 0.02, respectively. These values are very close to the fundamental anisotropies of TNP-ADP and MANT-ADP, indicating that the fluorophores attached to the ribose have very restricted motional freedom. Fluorescence of MANT-ADP free in solution decays with a nearly homogenous single lifetime of 3.9 ± 0.2 ns. However, upon binding, the emission is characterized by two components (τ_1 = 13.1 ± 0.5 ns, amplitude = 0.76, and τ_2 = 6.0 ± 0.2 ns, amplitude = 0.24). Very similar double-exponential fluorescence decays have been obtained with bound MANT-dADP and MANT-dATP. The data indicate that the chromophores attached to the ribose experience two different environments when bound to the DnaB helicase, which may reflect the existence of two different conformations of the ribose-binding region of the DnaB helicase nucleotide-binding site. This result is in contrast to a single environment and probably a lack of discrete conformational heterogeneity at the base-binding region, as probed by εADP fluorescence. Thus, the data indicate that conformational heterogeneity is localized around the ribose and not transmitted to the base-binding region, suggesting limited communication between base- and ribose-binding sites. The reported results provide the first insight into the nature of the significant structural differences between base- and ribose-binding regions of the nucleotide-binding site of the DnaB helicase. The importance of these differences, in terms of the biological functioning of the DnaB protein, is discussed.

The DnaB protein is a key replication protein in *Escherichia coli* (Kornberg & Baker, 1992), which is involved both in initiation and elongation stages of DNA replication and also plays a fundamental role in the replication of phage and plasmid DNA (McMacken et al., 1977; Ueda et al., 1978; Kaguni et al., 1982; Matson & Kaiser-Rogers, 1990). The protein is the *E. coli* primary replicative helicase, i.e., the factor responsible for unwinding the DNA duplex in front of

† This work was supported by NIH Grant R01 GM-46679 (to W.B.).

* Send correspondence to this author at Department of Human Biological Chemistry & Genetics, The University of Texas Medical Branch Galveston, 301 University Boulevard, Galveston, TX 77555-0653.

‡ On leave from Laboratory of Physical Chemistry, Drug Science Institute, Department of Pharmacy, Warsaw Medical School, Banacha 1, Warsaw, Poland.

® Abstract published in *Advance ACS Abstracts*, April 1, 1994.

0006-2960/94/0433-4682$04.50/0

the replication fork (LeBowitz & McMacken, 1986; Baker et al., 1987). DnaB protein is the only helicase required to reconstitute DNA replication *in vitro* from the chromosomal origin of replication (oriC). In its role as a "mobile replication promoter", DnaB protein binds to ssDNA.[1] The nucleoprotein complex is then specifically recognized by the primase (Arai & Kornberg, 1981b).

DnaB protein displays multiple activities *in vitro* which reflect its interactions with different ingredients in the primosome and the protein–nucleic acid complexes formed at the origins of bacterial and phage DNA replication. These activities include (1) binding of rNTPs (particularly ATP) and dNTPs (Arai et al., 1981a; Arai & Kornberg, 1981a–c; Reha-Krantz & Hurwitz, 1978b; Bujalowski & Klonowska, 1993), (2) ATPase and ribonucleotide triphosphatase activities (Arai & Kornberg, 1981a–c; Reha-Krantz & Hurwitz, 1978b; Bujalowski & Klonowska, 1993), (3) binding to ss- and dsDNA (Arai & Kornberg, 1981a,b; Reha-Krantz & Hurwitz, 1978b; LeBowitz & McMacken, 1986), (4) interactions with DnaC protein (Wahle et al., 1989a,b; Allen & Kornberg, 1991), primase (DnaG protein) (Arai & Kornberg, 1981b; LeBowitz & McMacken, 1986), phage λ-encoded P protein (Wickner, 1978; Mallory et al., 1990), and phage P1-encoded ban protein (Lanka et al., 1978), and (5) possible interactions with single-stranded binding (SSB) protein which strongly stimulates DnaB helicase activity (LeBowitz & McMacken, 1986).

In solution, the native DnaB protein exists as a stable hexamer composed of six identical subunits with a monomeric molecular weight of 52 265. The hexamer is most probably the species active *in vivo* (Arai et al., 1981a; Reha-Krantz & Hurwitz, 1978a; Bujalowski and Klonowska, submitted).

The binding, or binding and hydrolysis, of ATP is the key element regulating DnaB protein activities, including affinity toward nucleic acids and other components of the replication apparatus (Arai & Kornberg, 1981a–c; Arai et al., 1981b; Reha-Krantz & Hurwitz, 1978b; LeBowitz & McMacken, 1986). It has been proposed that ATP acts as a very specific positive allosteric effector which induces a conformational change in the protein and increases its affinity for ss nucleic acids. Moreover, the unwinding of duplex DNA by the DnaB helicase is fueled by the hydrolysis of ribonucleoside triphosphates, with ATP being the most efficient (LeBowitz & McMacken, 1986; Matson & Kaiser-Rogers, 1990).

It is clear that understanding the nucleotide interactions with DnaB protein, and its regulatory role, is indispensable for understanding different activities of the enzyme. Although the importance of the control and regulation of the DnaB protein functions by nucleotide phosphates has been recognized, the mechanism and the nature of this control still remain unknown at the molecular level.

Quantitative studies of the nucleotide binding to the DnaB helicase have established that the hexamer has six nucleotide-binding sites, presumably one on each protomer (Arai & Kornberg, 1981b; Bujalowski & Klonowska, 1993). On the basis of thermodynamically rigorous fluorescence titrations, we have determined that the binding process is biphasic, with the first three nucleotide molecules binding in the high-affinity step and the next three nucleotides binding in the low-affinity step. The biphasic behavior of binding isotherms results from the negative cooperative interactions among binding sites. The physiological role of the high- and low-affinity binding sites is still unknown. The statistical thermodynamic model, the hexagon, in which the negative cooperativity is limited to neighboring subunits, provides an excellent description of the binding process of nucleotides to the DnaB helicase (Bujalowski & Klonowska, 1993).

Early steady-state enzyme kinetic studies suggested significant differences between the base- and ribose-binding regions of the DnaB nucleotide-binding site in affecting the enzyme activities. Thus, the hydrolysis of nucleoside triphosphates, as well as the helicase activity, was relatively independent of the nature of the base (Arai & Kornberg, 1981a; LeBowitz & McMacken, 1986). On the other hand, DnaB could not hydrolyze either deoxynucleoside triphosphates or TNP-ATP, with a fluorescent group (TNP) attached to the 2′ and 3′ oxygens of the ribose (Arai & Kornberg, 1981a; Bujalowski & Klonowska, 1993). Also, the enzyme could not unwind duplex DNA in the presence of only deoxynucleotides, indicating intimate involvement of the sugar moiety of the nucleotide in the enzyme catalysis (LeBowitz & McMacken, 1986). Both γ-phosphate and intact ribose, but not the base moiety, appeared to be decisive elements in inducing allosteric interactions between the nucleotide and the ssDNA-binding site (Arai & Kornberg, 1981b; Bujalowski and Klonowska, manuscript in preparation). Clearly, different structural regions of the bound nucleotide molecule seem to be able to act either independently, triggering specific responses of the DnaB helicase through highly localized conformational changes, or together in a concerted way. In order to understand these complex interactions, the structure of the DnaB helicase nucleotide-binding site has to be determined.

In this communication, we describe the systematic studies of the structural characteristics of both the base- and ribose-binding regions of the high-affinity noninteracting nucleotide-binding site of the *E. coli* DnaB helicase, using different fluorescent nucleotide analogs: 1,N^6-ethenoadenosine diphosphate (εADP), 3′(2′)-*O*-(*N*-methylantraniloyl)adenosine 5′-diphosphate (MANT-ADP), 3′-*O*-(*N*-methylantraniloyl)-deoxyadenosine 5′-diphosphate (MANT-dADP), 3′-*O*-(*N*-methylantraniloyl)deoxyadenosine 5′-triphosphate (MANT-dATP), and 2′(3′)-*O*-(2,4,6-trinitrophenyl)adenosine 5′-diphosphate (TNP-ADP). These analogs differ by type and location of the modifying groups. In the case of TNP and MANT derivatives, the fluorescent groups are located on the ribose, while in the etheno derivative, the fluorescent modification is on the adenine residue (Bujalowski & Klonowska, 1993).

The obtained results provide the first characterization of the structural differences between the base- and ribose-binding regions of the nucleotide-binding site of the DnaB helicase. While the data indicate that the base is located in a rather polar environment and has relatively high motional freedom, the ribose is located in a hydrophobic region and has strongly constrained mobility. Solute quenching studies suggest that the base is significantly shielded but still has some access to the solvent. However, analogous studies suggest, within experimental accuracy, inaccessibility of the ribose-attached fluorophores to the solvent molecules. Moreover, fluorescence lifetime measurements of the MANT group indicate that the fluorophore senses two different environments, possibly two different conformations of the ribose-binding region. Only a single fluorescence lifetime was detected for the bound εADP,

[1] Abbreviations: TNP-ADP, 2′(3′)-*O*-(2,4,6-trinitrophenyl)adenosine 5′-diphosphate; εADP, 1,N^6-ethenoadenosine diphosphate; MANT-ADP, 3′(2′)-*O*-(*N*-methylantraniloyl)adenosine 5′-diphosphate; MANT-dADP, 3′-*O*-(*N*-methylantraniloyl)deoxyadenosine 5′-diphosphate; MANT-dATP 3′-*O*-(*N*-methylanttraniloyl)deoxyadenosine 5′-triphosphate; SSB, *E. coli* single-stranded binding protein; Tris, tris(hydroxymethyl)-aminomethane; ssDNA, single-stranded deoxyribonucleic acid; dsDNA, double-stranded deoxyribonucleic acid.

suggesting that the conformational heterogeneity around the ribose is not transmitted to the base-binding region of the nucleotide-binding site of the DnaB helicase.

MATERIALS AND METHODS

Reagents and Buffers. All chemicals were reagent grade. All solutions were made with distilled and deionized 18 MΩ (Milli-Q) water. The standard buffer (T2) was 50 mM Tris adjusted to pH 8.1 at appropriate temperatures with HCl, 5 mM $MgCl_2$, and 10% glycerol. The temperatures and the concentrations of NaCl in the buffer are indicated in the text.

Nucleotides. TNP-ADP was from Molecular Probes (Eugene, OR). The nucleotide was additionally purified, as described by Hiratsuka and Uchida (1973). εADP, from Sigma, was used without further purification. MANT-ADP, MANT-dADP, and MANT-dATP were synthesized by the method of Hiratsuka (1983). All nucleotides used in the binding studies were >95% pure as judged by TLC on silica.

DnaB Protein. The *E. coli* DnaB protein was purified from overproducing strain RLM1038, generously provided by Dr. Roger McMacken (Johns Hopkins University), using a slightly modified Arai–Kornberg procedure (Arai et al., 1981a; Bujalowski & Klonowska, 1993). The protein was >97% pure as judged by SDS polyacrylamide gel electrophoresis with Coomassie Brilliant Blue staining. The concentration of the protein was determined spectrophotometrically using the extinction coefficient $\epsilon_{280} = 1.85 \times 10^5$ cm^{-1} M^{-1} (hexamer) (Bujalowski and Klonowska, submitted).

Steady-State Fluorescence Measurements. All steady-state fluorescence measurements were performed using the SLM 48000S spectrofluorometer as we previously described (Bujalowski & Porschke, 1988a,b; Bujalowski & Klonowska, 1993). In the fluorescence intensity measurements, to avoid possible artifacts due to the fluorescence anisotropy of the sample, polarizers were placed in excitation and emission channels and set at 90° and 55° (magic angle), respectively. All steady-state intensity data were corrected, if necessary, for dilution and inner filter effects, using the following formula (Parker, 1968; Lakowicz, 1983)

$$F_{cor} = (F - B)(V/V_0)10^{0.5b(A_{\lambda ex})} \quad (1)$$

where F_{cor} is the corrected value of the fluorescence intensity, F is the experimentally measured fluorescence intensity, B is the background, V is the volume of the sample, V_0 is the initial volume of the sample, b is the total length of the optical path in the cuvette expressed in centimeters, and $A_{\lambda ex}$ is the absorbance of the sample at excitation wavelengths. The temperature of all measurements was controlled to ±0.1 °C.

Steady-State Fluorescence Anisotropy Measurements. All steady-state fluorescence anisotropy measurements were performed in L format using Glan-Thompson polarizers placed in the excitation and emission channel of the SLM 48000S spectrofluorometer. The fluorescence anisotropy of the sample was calculated using eq 2

$$r = (I_{VV} - GI_{VH})/(I_{vv} + 2GI_{VH}) \quad (2)$$

were I is the fluorescence intensity and the first and second subscripts refer to vertical (V) polarization of the excitation and vertical (V) or horizontal (H) polarization of the emitted light (Bujalowski & Lohman, 1989a,b). The factor $G = I_{HV}/I_{HH}$ corrects for the different sensitivity of the emission monochromator for vertically and horizontally polarized light (Azumi & McGlynn, 1962; Lakowicz, 1983).

Quantum Yield Determination. The quantum yields of free and bound nucleotide analogs, q_s, were determined by the comparative method of Parker and Reese (Parker & Reese, 1960) using the following relationship

$$q_S = q_R[(\int F_S \partial\lambda)10^{0.5b(A_S)}/(\int F_R \partial\lambda)10^{-0.5b(A_R)}](A_R/A_S) \quad (3)$$

where q_R is the quantum yield of a standard, $(\int F_S \partial\lambda)10^{0.5b(A_S)}$ and $(\int F_R \partial\lambda)10^{0.5b(A_R)}$ are the areas under the corrected emission spectra, corrected for inner filter effects of the standard and the fluorophore, respectively, A_S and A_R are the absorbances of the standard and the studied fluorophore at a given excitation wavelength, respectively, and b is the optical path in centimeters. Quinine bisulfate in 0.1 N H_2SO_4 was used as a reference for the excitations between 300 and 360 nm (absolute quantum yield $q_R = 0.7$; Scott et al., 1970), and fluorescein in 0.1 N NaOH was used for the excitation wavelength above 400 nm (absolute quantum yield $q_R = 0.92$; Weber & Teale, 1957).

Solute Accessibility Studies. Collisional, or dynamic, quenching of fluorescence results from random collisions between the quenching ligand Q and the fluorophore during the excited-state lifetime of the fluorophore (Parker, 1968; Lakowicz, 1983). If only the dynamic quenching process is present, the deactivation of the excited state of the fluorophore is described by eq 4 (Stern & Volmer, 1919)

$$F_0/F = 1 + K_{SV}[Q] \quad (4)$$

where F_0 and F are the steady-state fluorescence intensities in the absence and presence of the quenching ligand at concentration [Q]. K_{SV} is the Stern–Volmer quenching constant and is related to the bimolecular quenching rate constant k_q and to the fluorescence lifetime of the fluorophore τ by the relationship $K_{SV} = k_q\tau$.

The simultaneous presence of static and dynamic quenching processes may lead to the deviation from ideal Stern–Volmer behavior and can be closely approximated by (Lakowicz, 1983; Eftink, 1991)

$$F_0/F = (1 + K_{SV}[Q])\exp(V[Q]) \quad (5)$$

where V is the static quenching constant.

The efficiency of the solute quenching, γ, is a measure of the exposure of the bound fluorescent ligand and is defined as

$$\gamma = k_q^b/k_q^f \quad (6)$$

where k_q^b and k_q^f are the bimolecular quenching rate constants for bound and free fluorophores.

To obtain information about the accessibility and nature of the microenvironment surrounding different regions of the bound fluorescent nucleotide, quenchers having different physical properties have been selected. The quenching studies have been performed with neutral acrylamide, negatively charged iodide, I^-, and positively charged thallium, Tl^+ (Robbins et al., 1985; Philips et al., 1987; Eftink, 1991). As a control, titrations with ionic quenchers have also been performed in the presence of higher NaCl concentrations (~80 mM). No significant effect of the increased salt concentrations on determined quenching parameters has been observed.

Fluorescence Lifetime Measurements. Fluorescence lifetime determinations of nucleotide analogs, free and bound to

DnaB protein, have been performed using a SLM 48000S multifrequency, lifetime spectrofluorometer. Excitation was produced using a 450-W mercury–xenon lamp. The emission was detected through a Schott KV399-nm filter. To avoid fluorescence anisotropy artifacts in the phase-modulation measurements, Glan-Thompson polarizers were placed in excitation and emission channels and set at 90° and 55° (magic angle), respectively (Spencer & Weber, 1970). The modulation frequency was varied between 10 and 100 MHz at 1- and 2-MHz intervals. Usually, the data were collected for at least 50 different frequencies in a single experiment. The fluorescence lifetimes have been calculated from the phase shifts and demodulations of the emitted light from the sample with respect to scattered light from glycogen as a standard (τ = 0). The dependences of the phase shift and demodulation, as a function of the modulation frequency, were fitted to single or multiexponential decay functions, using the nonlinear least-squares fit routine provided by the manufacturer.

Determination of the Average Number of the Nucleotide Molecules Bound to DnaB Helicase. Studies described in this work focus on the structural characteristics of the high-affinity noninteracting nucleotide-binding site of the DnaB helicase (Bujalowski & Klonowska, 1993). In order to eliminate the interference of the free nucleotide on the fluorescence properties of the bound molecule, the concentrations of the protein and the nucleotide have to be selected to assure that the concentration of bound nucleotide [N_b] is practically equal to its total concentration [N_t]. Moreover, the average number of nucleotide analog molecules $(\sum\nu_i)_H$ bound per DnaB hexamer should not exceed 1.5–2.0 (see below). We previously described thermodynamic studies of the stoichiometries and the mechanism of nucleotide binding to the DnaB protein hexamer using fluorescent nucleotide analogs (Bujalowski & Klonowska, 1993). Using the rigorous thermodynamic method (Bujalowski & Lohman, 1987a,b), the absolute binding isotherms have been determined from fluorescence titrations, independent of the assumption of strict proportionality between the observed quenching of the protein fluorescence and the number of bound nucleotides (Bujalowski & Klonowska, 1993). The exact average number of given nucleotide analog molecules bound to DnaB protein $(\sum\nu_i)_H$ and the concentration of the bound nucleotide [N_b] used in this work have been calculated according to the hexagon model, using the intrinsic binding constants K's and the cooperativity parameters σ's, previously determined, according to the following equations (Bujalowski & Klonowska, 1993)

$$(\sum\nu_i)_H = (6x + 6(3 + 2\sigma)x^2 + 6(1 + 6\sigma + 3\sigma^2)x^3 + 12(3\sigma^2 + 2\sigma^3)x^4 + 30\sigma^4x^5 + 6\sigma^6x^6)/Z_H \quad (7a)$$

$$Z_H = 1 + 6x + 3(3 + 2\sigma)x^2 + 2(1 + 6\sigma + 3\sigma^2)x^3 + 3(3\sigma^2 + 2\sigma^3)x^4 + 6\sigma^4x^5 + \sigma^6x^6 \quad (7b)$$

$$[N_b] = (\sum\nu_i)H[\mathrm{DnaB}]_{total} \quad (7c)$$

where $x = K[N_f]$ and [N_f] is the free nucleotide concentration. $[\mathrm{DnaB}]_{total}$ is the total DnaB protein concentration in the sample. The quantity Z_H is the partition function of the DnaB hexamer–nucleotide system (Bujalowski & Klonowska, 1993).

RESULTS

Base-Binding Region of the Nucleotide-Binding Site of E. coli DnaB Protein. As we mentioned above, the subject of the studies in this work is the structural characterization of the high-affinity noninteracting nucleotide-binding site of the DnaB helicase. Binding of six nucleotides to the DnaB hexamer is described by a statistical thermodynamic model, the hexagon, in which the cooperative interactions are limited to neighboring binding sites (Bujalowski & Klonowska, 1993). Due to negative cooperativity, the binding process is biphasic, i.e., three molecules bind in the high-affinity step, and the subsequent three nucleotides bind in the low-affinity step.

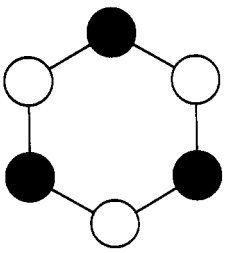

FIGURE 1: Schematic diagram showing the configuration of the hexagon with three high-affinity noninteracting sites of the DnaB hexamer saturated with ligand (closed circles). The statistical weight of this configuration is $2x^3$ (see eq 7b in the text).

This behavior of the binding process results from the fact that in the hexagon model, due to the low density of cooperative interactions, there will be a configuration with three nucleotide molecules bound which has much lower free energy than others with three nucleotides bound (see eq 7b; Bujalowski & Klonowska, 1993). This configuration is schematically presented in Figure 1 and corresponds to the situation where all three bound molecules are separated by an empty binding site (subunit), and hence, there are no cooperative interactions in this particular configuration of the hexamer–nucleotide system. If the degree of binding is low ($(\sum\nu_i)_H < 2$), then only the first terms in eq 7b, which do not contain σ, will have any significant contribution to the partition function of the system. Therefore, to eliminate possible interference of cooperative interactions, and to exclusively examine noninteracting high-affinity nucleotide-binding sites, all studies of bound nucleotides were performed on samples with the average number of nucleotide molecules bound per DnaB hexamer significantly lower than 2 (see below).

Corrected fluorescence emission spectra (λ_{ex} = 325 nm) of ϵADP free and bound to the DnaB helicase in buffer T2 (20 mM NaCl, pH 8.1, 20 °C) are shown in Figure 2a. In applied DnaB protein and nucleotide concentrations, >97% of ϵADP is bound. The average number of the bound nucleotide molecules $(\sum\nu_i)_H$ is ~0.11, thus assuring that, in the case of a protein–nucleotide complex, fluorescence properties of bound ϵADP in a noninteracting nucleotide-binding site are being examined. Binding of ϵADP to DnaB is accompanied by only a ~21% increase of the nucleotide fluorescence intensity, and there is no detectable shift of the maximum of the fluorescence spectrum, suggesting that the ethenoadenine-binding region has polarity similar to the bulk solvent (Sencrist et al., 1972; Spencer et al., 1974). This conclusion is further strongly supported by fluorescence lifetime measurements of the free and bound ϵADP. The emission of free ϵADP in buffer T2 (20 mM NaCl, pH 8.1, 20 °C) is characterized by a single lifetime, τ = 25.5 ± 0.6 ns (Table 1). The emission of ϵADP bound to DnaB is also characterized by a single lifetime, only ~5% shorter (τ = 24.2 ± 0.6 ns). Thus, binding of ϵADP to the DnaB helicase has little effect on the nucleotide fluorescence lifetime. This is in striking contrast to the effect of placing ϵADP in nonpolar solvents which causes a dramatic change in τ. The lifetime decreases from ~24 ns in water solution to ~15 ns in dioxane (Spencer et al., 1974). Thus, lack of a substantial change in ϵADP's lifetime, when bound

Table 1: Stern–Volmer Quenching Constants K_{SV}, Bimolecular Quenching Rate Constants k_q, Fluorescence Lifetimes τ, and Solute Quenching Efficiencies γ of ϵADP Free and Bound to DnaB Helicase in Buffer T2 (20 mM NaCl, pH 8.1, 20 °C)

nucleotide	quencher	quencher concentration (mM)	F_o/F	τ (ns)	τ_o/τ[a]	K_{SV} (M^{-1})	k_q[b] (M^{-1} s^{-1})	γ[c]
ϵADP (free)	acrylamide	0	1	25.5	1			
		30	2.43	11.2	2.28	47.7	2.19×10^9	
	I^-	0	1	25.5	1			
		30	5.10	6.2	4.10	136.5	5.3×10^9	
	Tl^+	0	1	25.5	1			
		30	3.84	6.7	3.8	94.7	4.8×10^9	
ϵADP (bound)	acrylamide	0	1	24.2	1			
		30	1.19	20.7	1.17	6.3	0.31×10^9	0.14
	I^-	0	1	24.2	1			
		30	1.71	14.8	1.64	23.5	1.16×10^9	0.22
	Tl^+	0	1	24.2	1			
		30[d]	1.75	14.0	1.73	24.9	1.32×10^9	0.28

[a] τ_o corresponds to the ϵADP lifetime determined in the absence of the quencher. [b] The values of k_q have been calculated using lifetime quenching data and corrected for the viscosity of the solvent (10% glycerol). [c] γ is defined by eq 6 (see text). [d] Because TlCl precipitates in our standard buffer (T2) at concentrations above ~8 mM, the titrations with Tl^+ have been performed in two buffer systems; in buffer T2 with Tl^+ concentration up to 5–6 mM and as a control in buffer (50 mM Tris/acetate, pH 8.1, 20 mM sodium acetate, 5 mM magnesium acetate, and 10% glycerol, 20 °C) with Tl^+ up to 35 mM. In the range of Tl^+ concentration from 0 to 6 mM, the quenching parameters as well as the fluorescence lifetimes were identical in both buffer systems. Binding of ϵADP is unaffected by the exchange of Cl^- for acetate in the buffer in the studied salt concentration range.

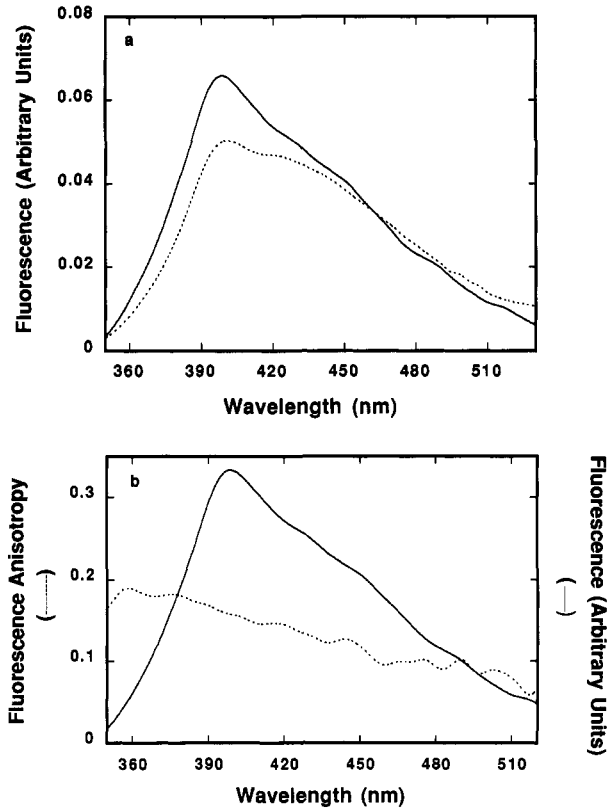

FIGURE 2: (a) Corrected fluorescence emission spectra of ϵADP (1.1×10^{-6} M) (– – –) free and bound (—) to DnaB helicase in buffer T2 (20 mM NaCl, pH 8.1, 20 °C); λ_{ex} = 325 nm. DnaB concentration is 1.0×10^{-5} M (hexamer). (b) Fluorescence anisotropy of ϵADP bound to DnaB helicase (– – –) as a function of emission wavelength; λ_{ex} = 325 nm, buffer T2 (20 mM NaCl, pH 8.1, 20 °C). The DnaB protein and ϵADP concentrations are 1.0×10^{-5} (hexamer) and 1.2×10^{-6} M, respectively. The emission spectrum (—) of the bound ϵADP recorded at the same excitation wavelength is also included.

to DnaB, strongly suggests polar character of the base-binding region in the nucleotide-binding site of the DnaB helicase.

Emission anisotropy of ϵADP bound to DnaB, as a function of emission wavelength, with the excitation at the red edge of the nucleotide absorption spectrum (λ_{ex} = 325 nm), is shown in Figure 2b. Although the accurate measurement of the anisotropy at both the blue and red sides of the emission spectrum is difficult, due to the low signal level in these regions, it is clear that the anisotropy varies significantly across the emission band, ranging from 0.18 ± 0.02 at 360 nm to 0.1 ± 0.02 at 500 nm (0.16 ± 0.01 at the maximum) (Figure 2b). Although this phenomenon has been observed before, it is still not completely understood (Gafni et al., 1979; Perkins et al., 1984). The fluorescence anisotropy of such a system is operationally defined by its value around the emission maximum (Sencrist et al., 1972; Perkins et al., 1984; Cheung & Liu, 1984). In the case of ϵADP bound to the DnaB helicase, the anisotropy at the emission maximum (~400–410 nm) r = 0.16 ± 0.01 is much lower than the anisotropy r_o = 0.3 ± 0.01 of completely immobilized ϵA at the same excitation and emission wavelengths (Sencrist et al., 1972; Cheung & Liu, 1984). However, it should be pointed out that bound ϵADP has a fluorescence lifetime of τ = 24.2 ns, which provides a long enough time window to observe rotational diffusion of the whole DnaB hexamer with a molecular weight of 313 590 (Nakayama et al., 1984a; Bujalowski & Klonowska, 1993). Thus, due to the rotation of the protein molecule, the observed anisotropy of bound ϵADP can be lower than its true limiting anisotropy. The effect of the protein rotational diffusion on the depolarization of bound ϵADP fluorescence can be estimated using the Perrin equation (Lakowicz, 1983)

$$r_{lim}/r = 1 + (\tau/\phi) \quad (8)$$

where r_{lim} is the limiting anisotropy of the bound ϵADP and $\phi = \eta V/RT$ is the rotational correlation time, η is the viscosity of the bulk solvent, R is the gas constant, and V is the volume of the protein molecule. Extrapolation of the Perrin plot (λ_{ex} = 325 nm, λ_{em} = 410 nm) to infinite viscosity, at constant temperature (20 °C), provides the limiting anisotropy of bound ϵADP r_{lim} = 0.21 ± 0.02 (plot not shown) (Table 3). As we mentioned above, the anisotropy of completely immobilized ϵA is r_0 = 0.3 ± 0.01 (λ_{ex} = 325 nm, λ_{em} = 410 nm), indicating that ethenoadenosine has substantial mobility when ϵADP is bound to the DnaB nucleotide-binding site (Sencrist et al., 1972; Cheung & Liu, 1984).

Solute Accessibility of the Adenine Ring in DnaB Helicase Nucleotide-Binding Site. Acrylamide, I^-, and Tl^+ are very effective quenchers of ethenoadenosine fluorescence (Ando & Asai, 1980; Perkins et al., 1984), differing dramatically in their physical properties. Acrylamide is a neutral molecule, while I^- and Tl^+, being significantly smaller than acrylamide, are negatively and positively charged, respectively. Fluorescence quenching studies using these quenchers should provide

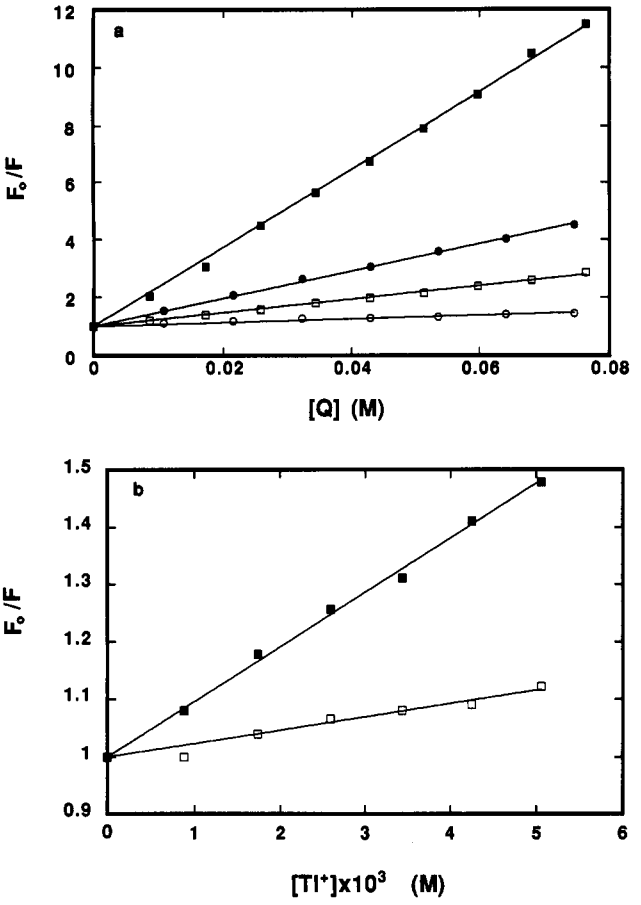

FIGURE 3: (a) Stern–Volmer plots of iodide and acrylamide quenching of the fluorescence of ϵADP free and bound to DnaB helicase in buffer T2 (20 mM NaCl, pH 8.1, 20 °C); λ_{ex} = 325 nm, λ_{em} = 450 nm. Iodide quenching: (■) free ϵADP and (●) bound ϵADP. Acrylamide quenching: (□) free ϵADP and (○) bound ϵADP. Solid lines are linear least-squares fits of Stern–Volmer equation (eq 4 in text) to the data points using the parameters included in Table 1; DnaB and ϵADP concentrations are 4.8 × 10^{-6} (hexamer) and 1.6 × 10^{-6} M, respectively. (b) Stern–Volmer plots of Tl^+ quenching of the fluorescence of ϵADP free and bound to DnaB helicase in buffer T2 (20 mM NaCl, pH 8.1, 20 °C); λ_{ex} = 325 nm, λ_{em} = 450 nm; (■) free ϵADP and (□) bound ϵADP. Solid lines are linear least-squares fits of Stern–Volmer equation (eq 4 in text) to the data points using the parameters included in Table 1; DnaB and ϵADP concentrations are 4.8 × 10^{-6} (hexamer) and 1.6 × 10^{-6} M, respectively.

the information not only on the accessibility of the adenine ring but also on the environment of the base location in the nucleotide-binding site (Eftink & Ghiron, 1981; Eftink, 1991; Robbins et al., 1985; Philips et al., 1987).

Stern–Volmer plots of fluorescence quenching of ϵADP, free and bound, in DnaB nucleotide-binding sites, as a function of acrylamide, I^-, and Tl^+ concentrations, are shown in Figure 3a,b. Fluorescence intensities and lifetimes of ϵADP in the presence of different quenchers, together with Stern–Volmer quenching constants K_{SV} and bimolecular quenching rate constants k_q, are included in Table 1. Stern–Volmer quenching constant K_{SV}, as well as bimolecular quenching rate constant k_q, for acrylamide is significantly lower than that determined for I^- and Tl^+. This is an expected result because of the larger size and slower diffusion of the acrylamide molecule compared to I^- and Tl^+. The lower values of K_{SV} and k_q may also reflect lower quenching efficiency of ethenoadenosine fluorescence compared to that of I^- and Tl^+, as previously indicated (Ando & Asai, 1980; Perkins et al., 1984). The bimolecular quenching rate constants for I^- and Tl^+ are close to the diffusion limits, with I^- being slightly more efficient.

In the case of acrylamide and I^-, the ratio of intensities F_o/F at a given quencher concentration is slightly higher than the corresponding ratio of lifetimes (Table 1). This result indicates that collisional quenching is predominant, as shown by the linear character of Stern–Volmer plots in Figure 3a. However, there is a small static component in the quenching mechanism of the fluorescence of free ϵADP by both quenchers.

Binding of ϵADP to the DnaB helicase nucleotide-binding site causes a dramatic decrease in the solute quenching efficiency of ϵADP fluorescence by studied quenchers as shown by Stern–Volmer plots in Figure 3 and quenching parameters included in Table 1. This effect is particularly pronounced in the case of acrylamide with K_{SV} and k_q values decreasing by a factor of ~7 compared to their values obtained for free ϵADP in solution. The corresponding quenching constants for I^- and Tl^+ decrease by factors of ~4.5 and ~3.6, respectively (Table 1). Linear Stern–Volmer plots (Figure 3), as well as $F_o/F \approx \tau_o/\tau$, indicate the collisional mechanism of the quenching processes of the bound nucleotide fluorescence.

The quenching data indicate that the solvent accessibility of the base's location in the DnaB nucleotide-binding site is limited. However, the fact that I^- and Tl^+, which are preferentially quenching surface-located chromophores, can still significantly quench the fluorescence of bound ϵADP suggests that the base is located in a cleft on the surface of the enzyme and preserves some limited access to the solvent (Lakowicz, 1983; Eftink, 1991).

It is interesting that I^- and Tl^+ both have very similar bimolecular quenching rate constants for bound ϵADP (Table 1). This result suggests that although the base binding site is polar, as indicated by fluorescence emission spectra and lifetime studies (see above), the distribution of the charges does not induce significant preference for quenchers having positive or negative charges.

Ribose-Binding Region of the Nucleotide-Binding Site of E. coli DnaB Helicase. To probe the structural environment around ribose-binding regions in the nucleotide-binding site of the DnaB helicase, we used ribose-modified fluorescent nucleotide analogs having TNP or MANT groups attached to the 2′ and/or 3′ oxygen of ribose rings (Bujalowski & Klonowska, 1993). Corrected fluorescence emission spectra (λ_{ex} = 408 nm) of TNP-ADP free and bound to a high-affinity noninteracting nucleotide-binding site of the DnaB helicase in buffer T2 (20 mM NaCl, pH 8.1, 20 °C) are shown in Figure 4a. Binding of the nucleotide analog is accompanied by a strong increase (by a factor of ~4.7) of its fluorescence intensity and quantum yield (Table 3). The emission spectra of free and bound TNP-ADP, normalized at the maximum, are shown in Figure 4b. The emission maximum shifts by ~11 nm from 563 nm for free to 552 nm for DnaB bound TNP-ADP.

The fluorescence properties of TNP nucleotide analogs are very sensitive to the solvent polarity and are suitable as reporters of the physical nature of the binding site (Hiratsuka, 1976). To obtain more information about the physical character of the ribose-binding region, as sensed by bound TNP-ADP, we recorded corrected fluorescence emission spectra of TNP-ADP, in solution, containing different concentrations of ethanol (Figure 5a). As the concentration of the ethanol in solution increases, the fluorescence intensity of the nucleotide analog strongly increases with concomitant shift of the emission maximum toward shorter wavelengths. It should be noted that both the intensity and the maximum of the emission spectrum change gradually with the change

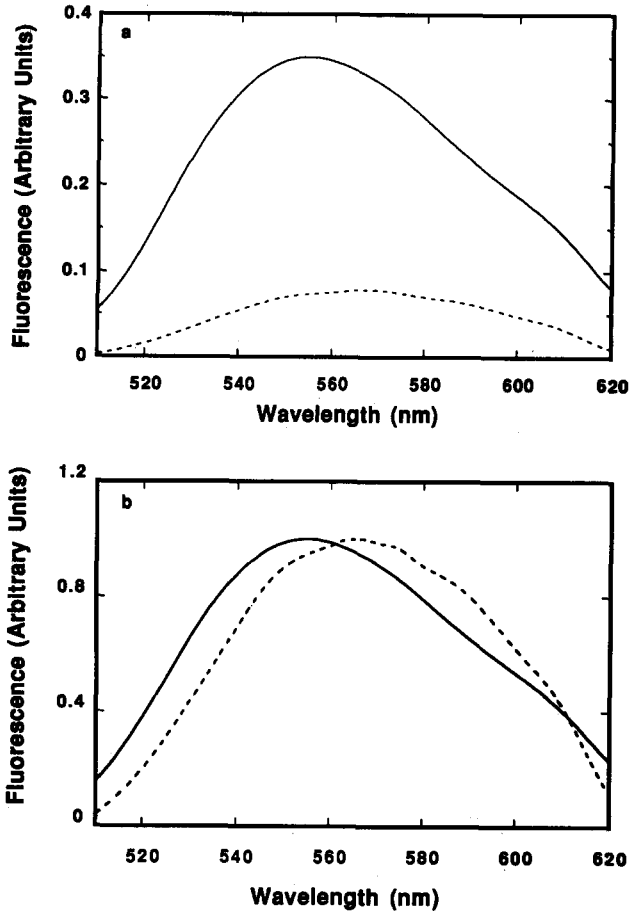

FIGURE 4: (a) Corrected fluorescence emission spectra of TNP-ADP (3.8×10^{-6} M) (- - -) free and bound (—) to DnaB helicase in buffer T2 (20 mM NaCl, pH 8.1, 20 °C); λ_{ex} = 408 nm. DnaB concentration is 4.8×10^{-6} M (hexamer). (b) Normalized corrected fluorescence emission spectra of TNP-ADP (3.8×10^{-6} M) (- - -) free and bound (—) to DnaB helicase in buffer T2 (20 mM NaCl, pH 8.1, 20 °C); λ_{ex} = 408 nm. DnaB concentration is 4.8×10^{-6} M (hexamer).

of the composition of the solvent, and there is no significant change in the shape of the emission spectrum, indicating that the general solvent effect is observed (Hiratsuka, 1976; Lakowicz, 1983). The dependence of the emission maximum and relative fluorescence intensity of TNP-ADP upon solvent polarity is shown in Figure 5b. The solvent polarity has been expressed, using Kosower's empirical polarity Z scale (Kosower, 1958; Turner & Brand, 1968). Both the location of the emission maximum and the emission intensity of the fluorescent analog show very good correlation with the Z value.

Although direct comparison should be treated with caution, the plot in Figure 5b may be used to estimate the Z value for the microenvironment surrounding the ribose-attached TNP group. The data for TNP-ADP bound to the DnaB helicase are included in Figure 5b (closed symbols). It should be noted that both the intensity and the emission maximum correspond to the very similar value of Z (90–90.8). The strong increase of TNP-ADP's fluorescence intensity and the blue shift of the emission maximum upon binding to DnaB protein strongly suggest that the ribose-binding site has a predominantly hydrophobic character which corresponds to a Z at ~90–90.8 on Kosower's empirical polarity scale.

Emission anisotropy of TNP-ADP bound to DnaB in buffer T2 (20 mM NaCl, pH 8.1, 20 °C), as a function of emission wavelength, with excitation at the red edge of the nucleotide absorption spectrum (λ_{ex} = 490 nm), is shown in Figure 6. The anisotropy is relatively constant throughout the spectrum,

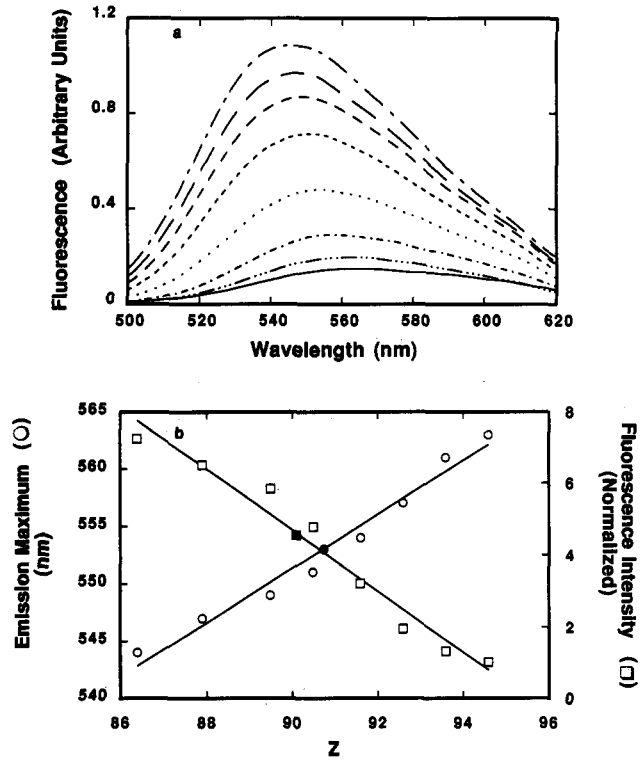

FIGURE 5: (a) Corrected fluorescence emission spectra of TNP-ADP in water solutions (1 mM Tris/HCl, pH 8.1, 25 °C) containing different concentrations of ethanol; λ_{ex} = 408 nm. TNP-ADP concentration is 1.96×10^{-5} M. Ethanol concentrations are (—) 0%, (—·—) 10%, (—··—) 20%, (···) 30%, (- - -) 40%, (- - -) 50%, (— — —) 60%, and (— - —) 70%. (b) Dependence of the position of the emission maximum (○) and the relative fluorescence intensity at the maximum (□) of TNP-ADP as a function of the solvent polarity expressed using Kosower's empirical polarity scale Z (Kosower, 1958; Turner & Brand, 1968). Solid lines are the linear least-squares fits to the data points. Closed symbols are the data obtained for TNP-ADP bound to DnaB protein (see Figure 4a,b).

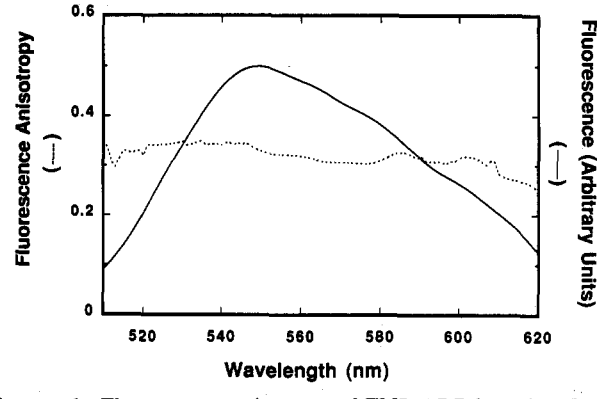

FIGURE 6: Fluorescence anisotropy of TNP-ADP bound to DnaB helicase (- - -) as a function of emission wavelength; λ_{ex} = 490 nm, buffer T2 (20 mM NaCl, pH 8.1, 20 °C). The DnaB protein and TNP-ADP concentrations are 4.8×10^{-6} (hexamer) and 3.8×10^{-6} m, respectively. The emission spectrum (—) of the bound TNP-ADP recorded in the same buffer conditions is also included.

although the error in this measurement is higher than in the case of ϵADP or MANT-ADP (see below), due to the low fluorescence intensity of the TNP-ADP. The emission anisotropy of the bound TNP-ADP, $r = 0.32 \pm 0.02$, is very close to its fundamental anisotropy, $r_o = 0.35$, at the same excitation wavelength (Moczydlowski & Fortes, 1981). This result indicates that when TNP-ADP is bound in the DnaB nucleotide-binding site, the ribose-attached TNP group has very limited motional freedom.

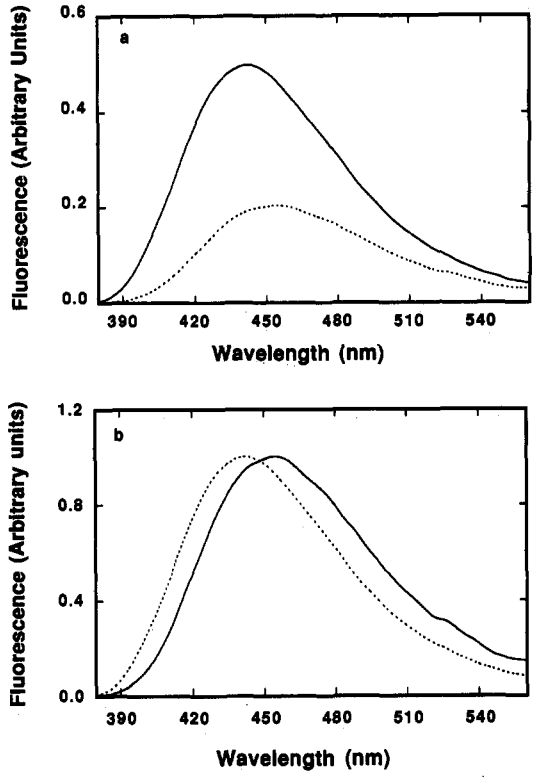

FIGURE 7: (a) Corrected fluorescence emission spectra of MANT-ADP (1.1×10^{-6} M) (- - -) free and bound (—) to DnaB helicase in buffer T2 (20 mM NaCl, pH 8.1, 20 °C); λ_{ex} = 356 nm. The DnaB concentration is 1.0×10^{-5} M (hexamer). (b) Normalized corrected fluorescence emission spectra of MANT-ADP (1.1×10^{-6} M) (—) free and bound (- - -) to DnaB helicase in buffer T2 (20 mM NaCl, pH 8.1, 20 °C); λ_{ex} = 356 nm. DnaB concentration is 1.0×10^{-5} M (hexamer).

The fluorescence properties of bound MANT-ADP corroborate well with the results obtained for TNP-ADP, described above. Corrected fluorescence emission spectra (λ_{ex} = 356 nm) of MANT-ADP free and bound to the DnaB helicase in buffer T2 (20 mM NaCl, pH 8.1, 20 °C) are shown in Figure 7a. As in the case of TNP-ADP, binding of the analog is accompanied by a dramatic increase in the fluorescence intensity (by a factor of ~2.7; see Table 3) and a large (~12 nm) blue shift of the emission spectrum (Figure 7b). These data indicate that, upon binding to DnaB, the MANT group has been placed in a hydrophobic environment (Hiratsuka, 1983; Cremo et al., 1990). The correlation between MANT-ADP fluorescence intensity and the position of the emission maximum with solvent polarity is similar to the one observed for TNP-ADP (data not shown). However, we could not follow the effect of solvent polarity on MANT-ADP fluorescence at higher (>50%) ethanol concentrations due to the significant propensity of this nucleotide analog to precipitate in these solution conditions.

Excitation fluorescence anisotropy spectra (λ_{em} = 450 nm) of MANT-ADP free and bound to the DnaB helicase in buffer T2 (20 mM NaCl, pH 8.1, 20 °C) are shown in Figure 8. Clearly, there is a dramatic change in the MANT-ADP fluorescence anisotropy accompanying the binding. For excitation in the region above 355 nm, anisotropy of the free MANT-ADP has a constant value of 0.015 ± 0.005. In the same excitation region, the anisotropy of the MANT-ADP bound to DnaB reaches the constant value of 0.33 ± 0.02. This value is close to the fundamental anisotropy of MANT-ADP, 0.35–0.4 (Cremo et al., 1990), indicating that the ribose-attached fluorophore has very constrained mobility.

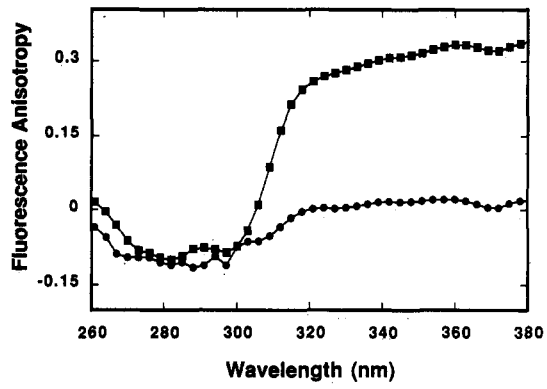

FIGURE 8: Excitation fluorescence anisotropy spectra of MANT-ADP free (●) and bound (■) to DnaB helicase in buffer T2 (20 M NaCl, pH 8.1, 20 °C); λ_{em} = 450 nm. The DnaB and MANT-ADP concentrations are 4.8×10^{-6} (hexamer) and 1.5×10^{-6} M, respectively.

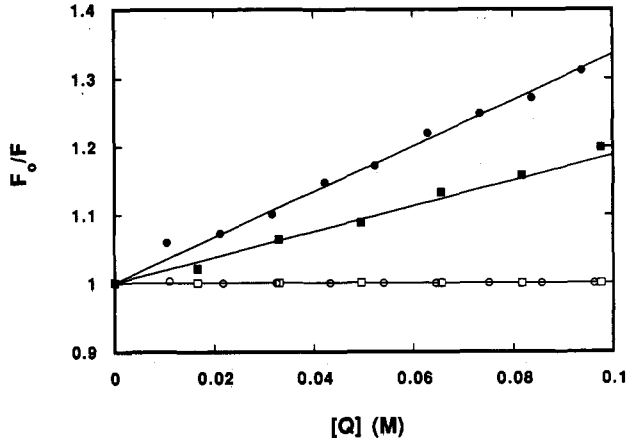

FIGURE 9: Stern–Volmer plots of iodide and acrylamide quenching of the fluorescence of MANT-ADP free and bound to DnaB helicase in buffer T2 (20 mM NaCl, pH 8.1, 20 °C); λ_{ex} = 356 nm, λ_{em} = 450 nm. Iodide quenching: (■) free MANT-ADP and (□) bound MANT-ADP. Acrylamide quenching: (●) free MANT-ADP and (○) bound MANT-ADP. DnaB and MANT-ADP concentrations are 4.8×10^{-6} (hexamer) and 1.0×10^{-6} M, respectively. Solid lines are linear least-squares fits of Stern–Volmer equation (eq 4 in text) to the data points using the parameters included in Table 2.

Solute Accessibility of the Ribose-Binding Region in DnaB Helicase Nucleotide-Binding Site. Accessibility of the ribose-attached fluorophore, free and bound to the DnaB nucleotide-binding site, to different solute quenchers has been determined using MANT-ADP. The analogous studies with TNP-ADP were hindered by the fact that the fluorescence lifetime of the TNP group is in the range of tens of picoseconds (Nakamoto & Inesi, 1984). This fluorescence lifetime is too short for solute quenching studies in the concentration ranges of the quenchers which do not perturb the equilibrium of nucleotide–DnaB protein interaction and/or the conformation of the enzyme (~0.08–0.1 M).

Stern–Volmer plots of the fluorescence quenching of MANT-ADP free and bound to DnaB nucleotide-binding sites as a function of acrylamide and KI concentrations are shown in Figure 9. The plots are linear within the range of acrylamide and KI concentrations studied, indicating the collisional character of the quenching process. The collisional mechanism of the quenching process is fully confirmed by the fluorescence lifetime studies of MANT-ADP in the presence of the studied quenchers (Table 2). The Stern–Volmer quenching constants obtained from steady-state intensity measurements are, within experimental error, identical to the quenching constants determined in lifetime experiments. This is expressed by the

Table 2: Stern–Volmer Quenching Constants K_{SV}, Bimolecular Quenching Rate Constants k_q, Fluorescence Lifetimes τ, and Solute Quenching Efficiencies γ of MANT-ADP Free and Bound to DnaB Helicase in Buffer T2 (20 mM NaCl, pH 8.1, 20 °C)

nucleotide	quencher	quencher concentration (mM)	F_0/F	τ (ns)	τ_0/τ[a]	K_{SV} (M^{-1})	k_q[b] (M^{-1} s^{-1})	γ[c]
MANT-ADP (free)	acrylamide	0	1.0	3.90	1.0			
		30	1.1	3.58	1.09	3.30	0.77×10^9	
	I^-	0	1.0	3.90	1.0			
		30	1.06	3.71	1.05	1.9	0.57×10^9	
	Tl^+	0	1.0	3.90	1.0			
		30	1.4	2.6	1.5	13.3	5.6×10^9	
MANT-ADP (bound)	acrylamide	0	1.0	6.0/13.1	1.0			
		30	1.0	6.0/13.1	1.0	~0	~0	~0
	I^-	0	1.0	6.0/13.1	1.0			
		30	1.0	6.0/13.1	1.0	~0	~0	~0
	Tl^+	0	1.0	6.0/13.1	1.0			
		30[d]	1.04	5.7/12.6	1.05/1.04	1.3	$0.27/0.14 \times 10^9$	0.05/0.030

[a] τ_0 corresponds to the MANT-ADP lifetime determined in the absence of the quencher. [b] The values of k_q have been calculated using lifetime quenching data and corrected for the viscosity of the solvent (10% glycerol). [c] γ is defined by eq 6 (see text). [d] Because TlCl precipitates in our standard buffer (T2) at concentrations above ~8 mM, the titrations with Tl^+ have been performed in two buffer systems; in buffer T2 with Tl^+ concentration up to 5–6 mM and as a control in buffer (50 mM Tris/acetate, pH 8.1, 20 mM sodium acetate, 5 mM magnesium acetate, and 10% glycerol, 20 °C) with Tl^+ up to 35 mM. In the range of Tl^+ concentration from 0 to 6 mM, the quenching parameters as well as the fluorescence lifetimes were identical in both buffer systems. Binding of MANT-ADP is unaffected by the exchange of Cl^- for acetate in the buffer in the studied salt concentration range.

Table 3: Fluorescence Properties of the Fluorescence Analogs ϵADP, MANT-ADP, MANT-dADP, and TNP-ADP Free and Bound to DnaB Helicase in Buffer T2 (20 mM NaCl, pH 8.1, 20 °C)

	ϵADP		MANT-ADP		MANT-dADP		TNP-ADP	
property	free	bound	free	bound	free	bound	free	bound
quantum[a] yield	0.53 ± 0.03	0.59 ± 0.03	0.22 ± 0.02	0.61 ± 0.03	0.27 ± 0.02	0.86 ± 0.05	$(7 \pm 2) \times 10^{-4}$	$(3.8 \pm 0.4) \times 10^{-3}$
limiting anisotropy	$(7 \pm 2) \times 10^{-3}$	0.21 ± 0.02[b]	0.015 ± 0.005	0.33 ± 0.02	0.016 ± 0.005	0.33 ± 0.02		0.32 ± 0.02
emission[a] maximum (nm)	400	400	453	441	452	442	563	552

[a] Excitation wavelengths for ϵADP, MANT-ADP, MANT-dADP, and TNP-ADP were 325, 356, 356 and 408 nm, respectively. [b] Determined from the extrapolation of isothermal Perin plot to infinite viscosity. The viscosity of the solvent has been changed using buffer T2 (20 mM NaCl, pH 8.1, 20 °C) containing different concentrations of glycerol (see eq 8 and the text for details). The controls have been performed to test that the increased glycerol concentration does not perturb DnaB–nucleotide equilibrium. The errors associated with the determination of quantum yields and limiting anisotropies are standard deviations obtained from three to four repeated measurements.

same value of the intensity F_0/F and lifetime τ_0/τ ratios at the corresponding quencher concentration (Table 2). It should be pointed out that the values of bimolecular quenching rate constants of free MANT-ADP fluorescence for all quenchers studied (acrylamide, I^-, and Tl^+) are lower than predicted by diffusion control quenching, an indication of the quenching process's low efficiency.

In contrast to the fluorescence of ϵADP bound to DnaB, which is still significantly quenched, particularly by I^- and Tl^+ (see Figure 3 and Table 1), within experimental accuracy, there is no detectable quenching of the MANT-ADP fluorescence bound to DnaB by acrylamide and I^-. In the case of Tl^+, the Stern–Volmer quenching constant is decreased by a factor of ~10 and the quenching efficiency by a factor of ~21, compared to the corresponding factor of ~3.6 for Tl^+ quenching of the bound ϵADP (Table 2). The larger drop of the quenching efficiency results from the fact that the lifetime of the bound MANT-ADP is significantly longer than that of free MANT-ADP (see below). Thus, these data strongly suggest that the accessibility of the ribose-binding region of the DnaB helicase nucleotide-binding site is significantly lower when compared to the solute accessibility of the base-binding region.

Fluorescence Lifetime of MANT-ADP Free and Bound to DnaB Helicase. Frequency–domain data of fluorescence decays of MANT-ADP free (closed symbols) and bound (open symbols) to DnaB protein in buffer T2 (20 mM NaCl, pH 8.1, 20 °C) are shown in Figure 10. As the modulation frequency increases, the phase angle increases and the modulation decreases. The data have been analyzed using the exponential decay laws, assuming ground-state heterogeneity (Lakowicz, 1983). The emission of free MANT-ADP

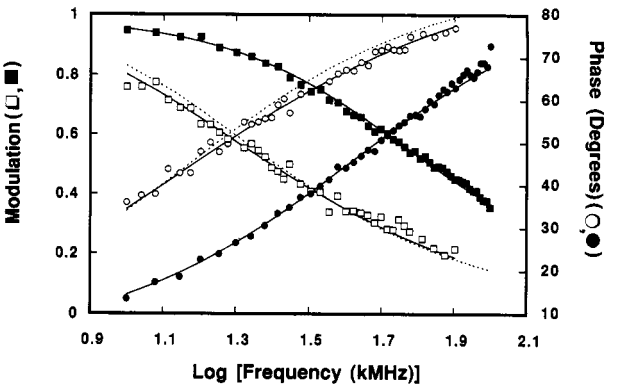

FIGURE 10: Frequency–domain, phase–modulation data for the fluorescence intensity decay of MANT-ADP free (closed symbols) and bound (open symbols) to DnaB helicase in buffer T2 (20 mM NACl, pH 8.1, 20 °C): (●) free MANT-ADP phase, (■) free MANT-ADP modulation, (○) bound MANT-ADP phase, and (□) bound MANT-ADP modulation. λ_{ex} = 356 nm (see Materials and Methods for experimental details). The solid lines are nonlinear double-exponential least-squares fits to the phase and modulation data using τ_1 = 3.9 ns, α_1 = 0.98, $\tau_2 > 20$ ns, and α_2 = 0.02 for free MANT-ADP and τ_1 = 6.0 ns, α_1 = 0.24, τ_2 = 13.1 ns, and α_2 = 0.76 for bound MANT-ADP, respectively (see Table 4). Dashed line represents a single exponential fit to phase–modulation data for bound MANT-ADP (τ = 10.5 ns); DnaB and MANT-ADP concentrations are 4.6×10^{-6} (hexamer) and 1.0×10^{-6} M, respectively.

in solution is almost exclusively characterized by a single lifetime, $\tau = 3.9 \pm 0.2$ ns (amplitude ~0.98). This value is in very good agreement with the previously determined 3.8 ns (Hiratsuka, 1984) and 4.06 ns (Cremo et al., 1990). Less than 2% of the total amplitude required a longer lifetime (>20 ns), which probably results from the presence of small buffer

Table 4: Fluorescence Lifetimes τ and Fractional Amplitudes α of MANT-ADP, MANT-dADP, and MANT-dATP Free and Bound to DnaB Protein Nucleotide-Binding Site (λ_{ex} = 356 nm) in Buffer T2 (20 mM NaCl, pH 8.1, 20 °C)[a]

	free				bound			
nucleotide	τ_1 (ns)	α_1	τ_2 (ns)	α_2	τ_1 (ns)	α_1	τ_2 (ns)	α_2
MANT-ADP	3.9 ± 0.2	0.97 ± 0.01	>20	0.03 ± 0.01	6.0 ± 0.2	0.24 ± 0.01	13.1 ± 0.5	0.76 ± 0.01
MANT-dADP	4.1 ± 0.2	0.98 ± 0.01	>20	0.02 ± 0.01	6.3 ± 0.2	0.27 ± 0.02	12.9 ± 0.5	0.73 ± 0.02
MANT-dATP	4.2 ± 0.2	0.97 ± 0.02	>20	0.03 ± 0.01	6.5 ± 0.2	0.28 ± 0.02	12.8 ± 0.5	0.72 ± 0.02

[a] The errors associated with the determination of lifetimes and amplitudes are standard deviations obtained from four to five repeated experiments.

impurities (Table 4). Binding of MANT-ADP to DnaB dramatically changes fluorescence lifetime characteristics of the nucleotide. The fluorescence decay of the bound nucleotide becomes biexponential with the shorter component characterized by τ_1 = 6.0 ± 0.2 ns and amplitude α = 0.24 and the longer component characterized by τ_2 = 13.1 ± 0.5 ns and α_2 = 0.76, respectively (see Figure 10 and Table 4). Including a third component did not significantly improve the statistics of the fit. For comparison, the fit with only a single decay time (τ = 10.5 ns) has been included (dashed line in Figure 10). We also performed phase–modulation studies of the fluorescence lifetime characteristics of MANT-dADP and MANT-dATP free and bound to the DnaB helicase. Within experimental accuracy, the lifetime characteristics of all studied MANT derivatives are very similar. The fluorescence of free nucleotide is characterized by a nearly homogeneous lifetime of ~4 ns, while, when bound to DnaB, the nucleotide emission is characterized by two decay times, ~6 and ~13 ns (Table 4).

The presence of two decay times in the emission of the bound nucleotides indicates that the MANT groups attached to the ribose sense two different environments, suggesting that the ribose-binding region of the nucleotide-binding site exists in two different conformations. Both lifetimes are much longer than the fluorescence lifetime obtained for free MANT derivatives (Table 4). This is in contrast to the result obtained for the base-binding region, where the single fluorescence lifetime of ϵADP very close to the lifetime of the free ϵADP was detected, indicating a lack of discrete conformational heterogeneity in the base-binding region. Thus, the data suggest that conformational heterogeneity of the ribose-binding region is not transferred to the base-binding site (see Discussion).

On the basis of chemical studies, MANT-ATP and MANT-ADP were originally postulated to exist solely as 3′ isomers (Hiratsuka, 1983). Recent NMR studies indicate that MANT-ATP and MANT-ADP may exist as a mixture of 2′ and 3′ isomers, with the 3′ isomer being predominant (Cremo et al., 1990). The single lifetime for this analog could result exclusively from the fraction of analog existing as the 3′ isomer with the 2′ isomer fraction being completely quenched. To test this possibility, we determined the quantum yield of MANT-ADP, MANT-dADP, and MANT-dATP. If there is a significant fraction of nonfluorescent 2′ isomer, the quantum yield of MANT-ADP should be lower when compared to the quantum yield of deoxy analogs by this fraction. The obtained data indicate that the quantum yield of MANT-ADP is indeed lower than that of MANT-dADP and MANT-dATP by ~19% (Table 3). Thus, it is possible that a lower quantum yield of MANT-ADP by ~19% compared to those of MANT-dADP and MANT-dATP reflects the existence of part of MANT-ADP in solution as a nonfluorescent 2′ isomer, as proposed originally by Cremo et al. (1990).

DISCUSSION

Binding of small ligands to biological macromolecules plays a crucial role in macromolecular activities (Schellman, 1975). In the case of proteins and nucleic acids, ligand binding can regulate both the thermodynamics and kinetics of the conformational stability and interactions (Bujalowski et al., 1986a,b; Bujalowski & Porschke, 1984, 1988a,b; Wong & Lohman, 1992). Regulation and control of multiple activities and interactions of *E. coli* DnaB protein are realized through binding and/or hydrolysis of nucleoside triphosphate molecules (Arai & Kornberg, 1981a,b; LeBowitz & McMacken, 1986; Wahle et al., 1989a,b; Bujalowski & Klonowska, 1993). Allosteric interactions between nucleotide-binding sites and different parts of the DnaB protein are the key elements in the enzyme action. It is clear that understanding the function of the DnaB protein requires understanding of the nature and structure of the nucleotide-binding sites and the conformation of the bound nucleotide.

Although treated as a "small" ligand, the nucleotide is a complex molecule with distinctive structural regions (base, ribose, phosphates), each of which can be responsible for triggering specific responses of the DnaB hexamer and control its activities either independently or in a concerted way. Thus, it has been shown that hydrolysis of nucleoside triphosphate is relatively independent of the nature of the base; however, the DnaB protein could not hydrolyze deoxynucleotides or the ribose-modified nucleotide TNP-ATP (Arai & Kornberg, 1981a; Bujalowski & Klonowska, 1993). Moreover, the presence of the γ-phosphate and the ribose is indispensable in inducing allosteric interactions between nucleotide- and ssDNA-binding sites. In the presence of ATP, or nonhydrolyzable ATP analogs, the affinity of DnaB for ssDNA is increased significantly, while no such effect has been observed in the presence of ADP or dATP (Arai & Kornberg, 1981a).

Application of fluorescent analogs can provide information about the binding mechanism, nature, structure, and dynamics of the nucleotide-binding site, unavailable by other approaches (Moczydlowski & Fortes, 1981; Perkins et al., 1984; Aguirre et al., 1989; Nakamoto & Inesi, 1984; Cremo et al., 1990; Bujalowski & Klonowska, 1993).

In this report, we probed the structural characteristics of the base- and ribose-binding regions of the high-affinity noninteracting nucleotide-binding site of the DnaB helicase, using fluorescent nucleotide analogs, which differ by type and location of the modifying group. To characterize the base-binding region, etheno-ADP, which has a modified adenine ring, has been used (Sencrist et al., 1972; Leonard, 1984, and references therein). To probe the region near the ribose-binding site, TNP-ADP and MANT-ADP, which have fluorescent groups trinitrophenyl (TNP) and methylantraniloyl (MANT) attached to the ribose 2′ and/or 3′ oxygens, have been selected.

The experiments reported in this work provide first insight into the nature of significant structural differences between base- and ribose-binding regions of the DnaB helicase's

nucleotide-binding site. Emission spectrum of εADP bound to a noninteracting binding site of the DnaB helicase shows only a slight increase in the nucleotide fluorescence intensity (~21%) and no detectable change in the position of the emission maximum as compared to that of free εADP in solution. Also, the fluorescence of the bound nucleotide is characterized by a single lifetime of 24.2 ± 0.6 ns, which is only ~5% shorter than the single lifetime of the free nucleotide (25.5 ± 0.6 ns; see Table 1). The effect of solvent polarity on fluorescence properties of ethenoadenosine derivatives has been intensively studied by Leonard and collaborators (Sencrist et al., 1972; Spencer et al., 1974; Leonard, 1984). In solvents of low polarity (e.g., dimethylformamide, dioxane), the fluorescence quantum yield decreases by ~15% with concomitant blue shift of the emission maxima. Moreover, the fluorescence lifetime of ethenoadenosine decreases significantly from 24 ns in H_2O (pH 7.0) to 15 ns in dioxane (Spencer et al., 1974).

Thus, the fluorescence properties of bound εADP strongly suggest that the base-binding region of the DnaB nucleotide-binding site has relatively high polarity, similar to the polarity of the bulk solvent. However, solute accessibility studies, using acrylamide, I^-, and Tl^+, indicate that bound adenine is significantly shielded from the solvent. Both Stern–Volmer quenching constants K_{SV} and bimolecular quenching rate constants k_q, for studied quenchers, are strongly decreased for bound εADP, compared to free nucleotide in solution. Within experimental accuracy, the quenching mechanism of bound εADP fluorescence is collisional. The lowest efficiency of quenching (0.14) is observed for neutral acrylamide, while negatively charged I^- and positively charged Tl^+ show similar quenching efficiency (0.22 and 0.28, respectively).

I^- and Tl^+ are similar in size and diffusion coefficients (Ando & Asai, 1980); thus, any significant difference in collisional quenching efficiency between these two ionic quenchers would result from differences in electrostatic interactions with the chromophore environment. Lack of significant differences between I^- and Tl^+ quenching efficiencies of bound εADP fluorescence suggests that the polar environment of the base-binding site has charge distribution, which does not provide strong preference for negatively or positively charged quenchers. The data indicate that a substantial decrease of the quenching constants of I^- and Tl^+ for bound εADP results from steric constraints at the adenine-binding site and, in effect, limited accessibility to the solvent. It should be pointed out that both ionic quenchers, I^- and Tl^+, are incapable of penetrating the protein matrix; hence, they preferentially quench surface-located chromophores (Lakowicz, 1983; Eftink, 1991). The fact that the fluorescence of bound εADP is still quenched by I^- and Tl^+ indicates that the adenine is located in the cleft on the surface of the enzyme and preserves some contact with the solvent. In this context, the lowest accessibility of bound εADP observed for acrylamide is expected because it has larger dimensions than I^- and Tl^+; thus, it should experience more steric constraints.

It is interesting that the adenine of bound εADP, although significantly shielded from the solvent, still retains substantial mobility as indicated by fluorescence anisotropy data. The limiting anisotropy r_{lim} of εADP bound to the DnaB helicase obtained from the isothermal Perrin plot is 0.21 ± 0.02 (λ_{ex} = 325 nm, λ_{em} = 410 nm). This value is significantly lower than the fundamental anisotropy, $r_o = 0.3 \pm 0.01$, characteristic for completely immobilized ethenoadenine at the same excitation and emission wavelengths (Sencrist et al., 1972; Cheung & Liu, 1984). If one assumes that this depolarization results from a motion of emission dipole over a surface of a cone, the half angle of the cone, $\Theta_c \approx 27°$, can be calculated, using the relationship $r_{lim}/r_o = [\cos \Theta_c(1 + \cos \Theta_c)]^2/2$, as derived by Kinosita et al. (1977). The fact that, when bound, the adenine retains significant mobility suggests the lack of short-range specific interactions between the protein matrix and the base in the base-binding site. Also, nucleotides having different base residues bind with similar intrinsic affinity to the DnaB helicase (Bujalowski and Klonowska, manuscript in preparation). Thus, the data indicate that the interactions in the base-binding site of the DnaB helicase are not unique for a specific base, which corroborates well with experimentally observed low base specificity of ATPase and helicase activities of the DnaB protein (Arai & Kornberg, 1981a; LeBowitz & McMacken, 1986).

As we mentioned above, the importance of the ribose region of the DnaB protein nucleotide-binding site for the enzyme catalysis was indicated in the early studies of DnaB activities (Arai & Kornberg, 1981a; LeBowitz & McMacken, 1986). Structural characteristics of the ribose region of the DnaB nucleotide-binding site have been probed using two different fluorescent nucleotide analogs, TNP-ADP and MANT-ADP (Hiratsuka & Uchida, 1973; Hiratsuka, 1983). There are contrasting differences between ribose- and base-binding regions of the DnaB helicase nucleotide-binding site. Fluorescence intensity of bound TNP-ADP increases by a factor of ~4.7 (λ_{ex} = 408 nm), and the maximum of the emission spectrum is blue-shifted by ~11 nm compared to that of free TNP-ADP in solution (see Figure 4 and Table 3). In the case of MANT-ADP, the corresponding increase of the fluorescence intensity is by a factor of ~2.6 and the blue shift of emission spectrum is by ~12 nm. Both TNP-ADP and MANT-ADP show good correlation between their fluorescence intensity and the positions of emission maximum with the solvent polarity, using the empirical solvent polarity Z scale as defined by Kosower (Kosower, 1958; Turner & Brand, 1968). Thus, these results indicate that the environment near the ribose-binding site has a predominantly hydrophobic character.

Solvent accessibility studies indicate that the MANT group attached to the ribose has very little, if any, solvent accessibility when MANT-ADP is bound in the DnaB helicase nucleotide-binding site. In the case of acrylamide and I^-, the Stern–Volmer quenching constant K_{SV} is ~0 (Table 2). Quenching efficiency for Tl^+ is detectable (~0.05), suggesting the presence of negatively charged amino acid groups near the ribose-binding region. At this point, it should be noted that solute quenching studies of the fluorescence of DnaB tryptophans, which are located in/close to the nucleotide-binding site, also show strong preferential quenching by Tl^+, compared to I^- (Bujalowski and Klonowska, submitted). Thus, the data suggest that protein tryptophans may constitute part of the hydrophobic microenvironment around the ribose-binding region.

Fluorescence anisotropy of MANT-ADP and TNP-ADP bound to DnaB is 0.33 ± 0.02 and 0.32 ± 0.02, respectively. The values are very close to the fundamental anisotropies of these nucleotide analogs, ~0.35–0.4, indicating that both fluorophores attached to the ribose have very limited motional freedom (Moczydlowski & Fortes, 1981; Cremo et al., 1990). These results are particularly interesting in the case of MANT-ADP, whose major emission component (fractional amplitude = 0.76) decays with a lifetime of 13.1 ± 0.5 ns (Table 4). This is a time window long enough to sense rotational motion with correlation time up to ~50 ns (Lakowicz, 1983). Thus, the data strongly suggest that the entire ribose-binding region

has substantially limited mobility with respect to the protein matrix.

Fluorescence of MANT-ADP, free in solution, decays with a nearly homogeneous single lifetime of 3.9 ± 0.2 ns (buffer T2, 20 mM NaCl, pH 8.1, 20 °C) which is very similar to the values previously obtained by Cremo et al. (4.06 ns) and Hiratsuka (3.8 ns) (Cremo et al., 1990; Hiratsuka, 1983). Very similar values of fluorescence lifetimes have been obtained for MANT-dADP and MANT-dATP (Table 4). Binding to the DnaB helicase induces dramatic changes in the MANT-ADP emission decay characteristics. The decay becomes heterogeneous and is described by two components, $\tau_1 = 6.0 \pm 0.2$ ns (amplitude 0.24) and $\tau_2 = 13.1 \pm 0.5$ ns (amplitude 0.76). Thus, both fluorescence lifetimes are increased with respect to the lifetime of free MANT-ADP. The presence of two lifetimes is not a result of the possible different locations of the MANT group in 2′ and 3′ isomers in the ribose-binding region. Both MANT-dADP and MANT-dATP, which have a MANT group attached exclusively to the 3′ oxygen show, within experimental accuracy, the presence of the same two decay components (Table 4). The fluorescence lifetime is a very sensitive measure of the heterogeneity of the environment surrounding the fluorophore (Lakowicz, 1983). The presence of two lifetimes for the MANT-ADP, MANT-dADP, and MANT-dATP bound to the DnaB helicase strongly suggests that the chromophore experiences two different environments, possibly two different conformations, of the ribose-binding region of the DnaB helicase nucleotide-binding site. This result is in contrast to a single environment and probably to a lack of discrete conformational heterogeneity at the base-binding region, as probed by εADP fluorescence. The data indicate that conformational heterogeneity is localized in the ribose-binding region and that it is not transmitted to the base-binding region, suggesting limited communication between base- and ribose-binding sites.

DnaB helicase is a free-energy transducing enzyme which can catalyze the unwinding of duplex DNA fueled by ATP hydrolysis (LeBowitz & McMacken, 1986; Baker et al., 1987). A common feature of such enzymes is that they undergo a conformational transition in their active sites during the catalysis (Hill, 1977). To our knowledge, no data are available on the nature and conformation of the nucleotide-binding sites of other helicases. Therefore, comparison of results obtained in this work on the DnaB helicase to the functionally and/or structurally homologous enzymes is not possible at this time. However, the energetics of the two-state conformational transition of the ATP-binding site have been characterized in the case of the other free-energy transducing system, the myosin subfragment S-1, and were proposed to be involved in the "power stroke" of the contractile cycle (Shriver & Sykes, 1982; Aguirre et al., 1989; Lin & Cheung, 1990). It is possible that conformational heterogeneity in the ribose-binding region of the DnaB helicase nucleotide-binding site, described in this work, reflects conformational changes involved in the "power stroke" in the DnaB helicase action (Hill & Tsuchiya, 1982).

ACKNOWLEDGMENT

We would like to thank Drs. D. Wayne Bolen and Edmund W. Czerwinski for careful reading and comments on the manuscript. We would also like to thank Mrs. Gloria Drennan Davis for help in preparing the manuscript.

REFERENCES

Aguirre, R., Lin, S. H., Gonsoulin, F., Wang, C. K., & Cheung, H. C. (1989) *Biochemistry 28*, 799–807.

Allen, G. C., & Kornberg, A. (1991) *J. Biol. Chem. 266*, 22096–22101.

Ando, T., & Asai, H. (1980) *J. Biochem. 88*, 255–264.

Arai, K., & Kornberg, A. (1981a) *J. Biol. Chem. 256*, 5253–5259.

Arai, K., & Kornberg, A. (1981b) *J. Biol. Chem. 256*, 5260–5266.

Arai, K., & Kornberg, A. (1981c) *J. Biol. Chem. 256*, 5267–5272.

Arai, K., Yasuda, S., & Kornberg, A. (1981a) *J. Biol. Chem. 256*, 5247–5252.

Arai, K., Low, R., Kobori, J., Shlomai, J., & Kornberg, A. (1981b) *J. Biol. Chem. 256*, 5273–5280.

Azumi, T., & McGlynn, S. P. (1962) *J. Chem. Phys. 37*, 2413–2420.

Baker, T. A., Funnell, B. E., & Kornberg, A. (1987) *J. Biol. Chem. 262*, 6877–6885.

Bujalowski, W., & Porschke, D. (1984) *Nucleic Acids Res. 12*, 7549–7563.

Bujalowski, W., & Lohman, T. M. (1987a) *Biochemistry 26*, 3099–3106.

Bujalowski, W., & Lohman, T. M. (1987b) *J. Mol. Biol. 195*, 897–907.

Bujalowski, W., & Porschke, D. (1988a) *Biophys. Chem. 30*, 151–157.

Bujalowski, W., & Porschke, D. (1988b) *Z. Naturforsch. 43c*, 91–98.

Bujalowski, W., & Lohman, T. M. (1991a) *J. Biol. Chem. 266*, 1616–1626.

Bujalowski, W., & Lohman, T. M. (1991b) *J. Mol. Biol. 217*, 63–74.

Bujalowski, W., & Klonowska, M. M. (1993) *Biochemistry 32*, 5888–5900.

Bujalowski, W., Greaser, E., McLaughlin, W., & Porschke, D. (1986a) *Biochemistry 25*, 6365–6371.

Bujalowski, W., Jung, M., McLaughlin, W., & Porschke, D. (1986b) *Biochemistry 25*, 6372–6378.

Cheung, H. C., & Liu, B. M. (1984) *J. Muscle Res. Cell Motil. 5*, 65–80.

Cheung, H. C., Gonsoulin, F., & Garland, F. (1985) *Biochim. Biophys. Acta 832*, 52–62.

Cremo, C. R., Neuron, J. M., & Yount, R. G. (1990) *Biochemistry 29*, 3309–3319.

Eftink, M. R. (1991) in *Biophysical and Biochemical Aspects of Fluorescence Spectroscopy* (Dewey, T. C., Ed.) Chapter 1, Plenum Press, New York, London.

Eftink, M. R., & Ghiron, C. A. (1981) *Anal. Biochem. 114*, 199–227.

Gafni, A., Schlessinger, J., & Steinberg, I. Z. (1979) *J. Chem. Soc. 101*, 463–467.

Hill, T. L. (1977) *Free Energy Transduction in Biology*, Academic Press, New York.

Hill, T. L., & Tsuchiya, T. (1981) *Proc. Natl. Acad. Sci. U.S.A. 78*, 4796–4800.

Hiratsuka, T. (1983) *Biochim. Biophys. Acta 742*, 496–508.

Hiratsuka, T. (1984) *J. Biochim. 96*, 155–162.

Hiratsuka, T., & Uchida, K. (1973) *Biochim. Biophys. Acta 320*, 635–647.

Kaguni, J. M., Fuller, R. S., & Kornberg, A. (1982) *Nature 296*, 623–626.

Kinosita, K., Jr., Kawato, S., & Ikegami, A. (1977) *Biophys. J. 20*, 289–305.

Kornberg, A., & Baker, T. A. (1992) *DNA Replication*, Freeman, San Francisco.

Kosower, E. M. (1958) *J. Am. Chem. Soc. 80*, 3253–3260.

Lakowicz, J. R. (1983) *Principle of Fluorescence Spectroscopy*, Chapter 10, Plenum Press, New York, London.

Lanka, E., Geschke, B., & Schuster, H. (1978) *Proc. Natl. Acad. Sci. U.S.A. 75*, 799–803.

LeBowitz, J. H., & McMacken, R. (1986) *J. Biol. Chem. 261*, 4738–4748.

Leonard, N. J. (1984) *Crit. Rev. Biochem. 15*, 125–199.

Lin, S. H., & Cheung, H. C. (1989) *Biochemistry 30*, 4317–4322.
Mallory, J. B., Alfano, C., & McMacken, R. (1990) *J. Biol. Chem. 265*, 13297–13307.
Matson, S. W., & Kaiser-Rogers, K. A. (1990) *Annu. Rev. Biochem. 59*, 289–329.
McMacken, R., Ueda, K., & Kornberg, A. (1977) *J. Biol. Chem. 253*, 3313–3319.
Moczydlowski, E. G., & Fortes, P. A. G. (1981) *J. Biol. Chem. 256*, 2346–2356.
Nakamoto, R. K., & Inesi, G. (1984) *J. Biol. Chem. 259*, 2961–2970.
Nakayama, N., Arai, N., Kaziro, Y., & Arai, K. (1984a) *J. Biol. Chem. 259*, 88–96.
Nakayama, N., Arai, N., Bond, M. W., Kaziro, Y., & Arai, K. (1984b) *J. Biol. Chem. 259*, 97–101.
Parker, C. A. (1968) *Photoluminescence of Solutions*, Elsevier Publishing Co., Amsterdam.
Parker, C. A., & Reese, W. T. (1960) *Analyst 85*, 587–592.
Perkins, W. J., Wells, J. A., & Yount, R. G. (1984) *Biochemistry 23*, 3994–4002.
Philips, A. V., Robbins, D. J., Coleman, M. S., & Barkley, M. D. (1987) *Biochemistry 26*, 2893–2903.
Reha-Krantz, L. J., & Hurwitz, J. (1978a) *J. Biol. Chem. 253*, 4043–4050.
Reha-Krantz, L. J., & Hurwitz, J. (1978b) *J. Biol. Chem. 253*, 4051–4057.
Robbins, D. J., Deibel, M. R., Jr., & Barkley, M. D. (1985) *Biochemistry 24*, 7250–7257.
Schekman, R., Weiner, A., & Kornberg, A. (1974) *Science 186*, 987–993.
Schekman, R., Weiner, J. H., Weiner, A., & Kornberg, A. (1975) *J. Biol. Chem. 250*, 5859–5865.
Schellman, J. (1975) *Biopolymers 14*, 999–1018.
Scott, T. G., Spencer, R. D., Leonard, N. J., & Weber, G. (1970) *J. Am. Chem. Soc. 92*, 687–695.
Secrist, J. A., Bario, J. R., Leonard, N. J., & Weber, G. (1972) *Biochemistry 11*, 3499–3506.
Shriver, J. W., & Sykes, B. D. (1982) *Biochemistry 21*, 3022–3028.
Spencer, R. D., & Weber, G. (1970) *J. Chem. Phys. 52*, 1654–1663.
Spencer, R. D., Weber, G., Tolman, G., Barrio, J. R., & Leonard, N. J. (1974) *Eur. J. Biochem. 45*, 425–429.
Stern, O., & Volmer, M. (1919) *Phys. Z. 20*, 183–188.
Tanford, C. (1961) *Physical Chemistry of Macromolecules*, J. *Wiley*, New York.
Turner, D. C., & Brand, L. (1968) *Biochemistry 10*, 3381–3390.
Ueda, K., McMacken, R., & Kornberg, A. (1978) *J. Biol. Chem. 253*, 261–269.
Wahle, E., Lasken, R. S., & Kornberg, A. (1989a) *J. Biol. Chem. 264*, 2463–2468.
Wahle, E., Lasken, R. S., & Kornberg, A. (1989b) *J. Biol. Chem. 264*, 2469–2475.
Weber, G., & Teale, F. W. J. (1957) *Trans. Faraday Soc. 53*, 646–655.
Wickner, S. H. (1978) *Cold Spring Harbor Symp. Quant. Biol. 43*, 303–310.
Wickner, S., Wright, M., & Hurwitz, J. (1973) *Proc. Natl. Acad. Sci. U.S.A. 71*, 783–787.
Wong, I., & Lohman, T. M. (1992) *Science 256*, 350–355.